Bangladesh J. Bot. **55**(1): 133-143, 2026 (March) DOI: https://doi.org/10.3329/bjb.v55i1.88612

MORPHOLOGICAL PLASTICITY, ANATOMICAL FITNESS, AND YIELD-STRUCTURE COUPLING STABILITY IN OPTIMIZING IRRIGATION FOR WATER-SUSTAINABLE *PENNISETUM PURPUREUM* FORAGE PRODUCTION

SHIMOU HUANG*

Mongolian University of Life Sciences School of Economics and Business, Mongolia Ulaanbaatar

Keywords: Irrigation system, Forage production, *Pennisetum purpureum*, Water resource allocation, Morphological and anatomical response

Abstract

In forage production, addressing the issues of yield fluctuations and unclear structural adaptability of *Pennisetum purpureum* caused by uneven water resource allocation, this paper employs multi-gradient irrigation control combined with anatomical analysis. By precisely regulating water supply and simultaneously analyzing the dynamic response of tissue structure, the morphological basis for high and stable yields of *P. purpureum* under water-saving conditions is effectively revealed. This article sets four irrigation levels of 100, 75, 50, and 25% ETc, and systematically monitors morphological parameters such as plant height, tiller number, stem thickness, leaf area index, and dry matter accumulation. Combined with the microstructure quantification of leaf and stem cross-sections, a four-dimensional evaluation system for WUE, morphological plasticity index, anatomical fitness, and yield structure coupling stability was constructed. WUE of *P. purpureum* is highest under 75% ETc treatment, and tillering ability was not inhibited but rather enhanced. Under 50% ETc conditions, the ratio of leaf palisade tissue/sponge tissue significantly increased, while the proportion of stem vascular bundles remained stable, indicating the synergistic optimization of photosynthesis and transport functions. The yield of hay is positively correlated with the proportion of stem thick walled cells ($r>0.7$), and this structural parameter fluctuates less than 10% under various water deficit treatments, confirming that it is a key anatomical guarantee for stable yield. The results indicate that *P. purpureum* can maintain forage productivity through morphological compensation and tissue restructuring under moderate water deficit, and has the potential to be promoted as a water-saving forage crop.

Introduction

Pennisetum purpureum is a major forage resource in tropical and subtropical regions due to its high productivity, rapid growth rate, and substantial biomass accumulation, which collectively ensure stable feed supply for animal production systems (Mohamad *et al.* 2022, Johannes *et al.* 2024). As agricultural water resources become increasingly limited, understanding the adaptive growth mechanisms of this species under different water regimes has become essential for optimizing irrigation strategies and improving water use efficiency (Ikpeseni *et al.* 2024). The morphological characteristics and internal tissue organization of elephant grass are closely associated with photosynthetic performance, water transport efficiency, and mechanical stability, thereby constituting intrinsic determinants of forage yield and quality stability (Ho *et al.* 2023). A comprehensive analysis of water-driven structural reorganization not only facilitates the identification of traits suitable for water-saving and stable production systems (Dios-León *et al.* 2022, Clark *et al.* 2023) but also provides a theoretical basis for establishing structure-oriented forage management frameworks, contributing to the sustainable development of grassland based animal agriculture.

*Author for correspondence: <hsm362826@163.com>.

Despite its agronomic importance, research on moisture responses in grasses remains fragmented. Many studies treat irrigation as a linear factor influencing yield or biomass accumulation, while overlooking the mechanistic processes by which plants maintain function through coordinated organ and tissue adjustment along water gradients (Rahman *et al.* 2025). Such output-oriented evaluation approaches cannot adequately explain the capacity of *P. purpureum* to sustain relatively stable forage yields under moderate water deficit conditions (Braga *et al.* 2022). Morphological parameters represent surface-level responses and fail to capture the internal functional dynamics supporting these phenotypes (Oluwadele *et al.* 2024). In contrast, anatomical traits, including the ratio of palisade to spongy mesophyll in leaves, vascular bundle density and distribution in stems, and the extent of sclerenchyma development, directly influence photosynthetic efficiency, hydraulic conductivity, and structural strength. However, these functional tissues have largely been excluded from conventional irrigation evaluation systems (Rahman *et al.* 2025).

Existing research lacks an integrated "structure–function–yield" analytical framework, which constrains irrigation design to empirical approaches and limits the accurate identification of critical water stress thresholds (Maldonado-Méndez *et al.* 2023, Putra *et al.* 2024). Morphological plasticity is often broadly characterized as strong adaptability without distinguishing the sensitivity of specific organs and tissues to water signals or quantifying the limits of compensatory regulation (Ikpeseni *et al.* 2025). In addition, experimental designs frequently rely on extreme water treatments, neglecting the transitional moisture intervals that are most relevant for balancing water conservation with production stability (Qohar *et al.* 2023). As a result, irrigation management decisions are often made without an anatomical basis, restricting the potential for promoting elephant grass as an efficient forage crop in water-limited environments.

Previous investigations into grass water responses have predominantly emphasized physiological and ecological dimensions, including photosynthetic rate, transpiration efficiency, water use efficiency, and root distribution patterns (de Oliveira Gonçalves *et al.* 2022). Morphological responses are commonly documented through measurements of plant height, tiller density, or leaf area index as indirect indicators of stress adaptation (Mijena and Getiso 2024). Although some anatomical observations have examined specific tissues (Silva *et al.* 2023), systematic quantification of functional tissues across gradient water treatments remains limited. While varietal differences and yield responses under field conditions have been reported (Mijena *et al.* 2023), a standardized system of structural indicators spanning multiple organs and treatments has not been established, thereby reducing comparability across studies. Moreover, morphology and anatomy are often regarded as passive outcomes of stress rather than active regulatory mechanisms supporting functional maintenance.

This study examines the coordinated responses of *P. purpureum* to graded irrigation (100-25% ETc), integrating morphological and microanatomical analyses. It aims to identify structural indicators of water-adaptive performance and establish a structure-yield framework to support precision irrigation and sustainable forage production under water-limited conditions.

Materials and Methods

The technical framework illustrated in Fig. 1 was designed to analyze the water adaptability of *P. purpureum* under water-saving irrigation. Based on regulated water resource allocation, a four-level irrigation gradient was established to precisely manipulate plant water supply. In response to this gradient, plants exhibited coordinated morphological and anatomical adjustments. At the macroscopic level, time-dependent changes occurred in plant heightker, tiller number, stem diameter, leaf area index (LAI), and dry matter accumulation (Jabessa *et al.* 2022, Veraque *et al.*

2023). At the microscopic scale, remodeling of leaf tissues and optimization of stem supporting structures were observed (Kalebbi *et al.* 2024, Ikyume *et al.* 2025). These datasets were integrated into a multidimensional analytical system encompassing resource-use efficiency, morphological plasticity, anatomical robustness, and structural yield stability, ultimately identifying drought-tolerant anatomical traits and optimal irrigation thresholds for stable forage production.

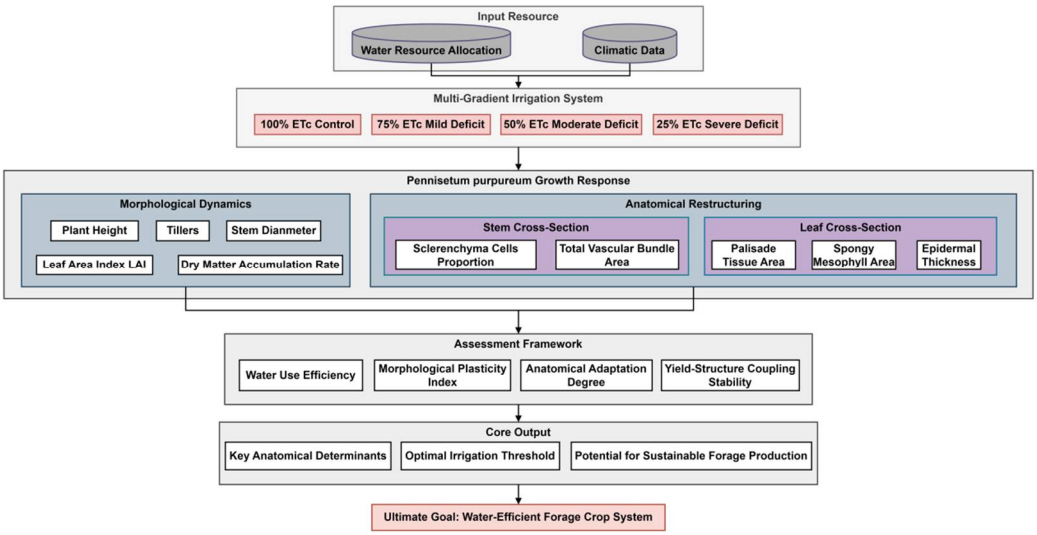

Fig. 1 Multidimensional analytical system for studying water adaptability of *Pennisetum purpureum*.

A multi-gradient irrigation regime was established based on crop evapotranspiration (ETc). Full irrigation (100% ETc) served as the control, while mild, moderate, and severe deficits were set at 75, 50 and 25% ETc, respectively. Irrigation volumes were dynamically adjusted according to meteorological data and crop growth stage. A drip irrigation system equipped with pressure-compensated emitters ensured water delivery accuracy within ±5%. Treatments were arranged in a randomized layout with three independent replicates (plot size 120 m^2), maintaining ≥2 m spacing between plots to prevent lateral water movement. Plant spacing was 0.8 × 0.4 m.

Soil moisture sensors (EC-5; reet sampling frequency 1 h^{-1}) provided feedback control. When soil moisture deviated by more than ±3% from preset values, an automated correction program restored target levels. Irrigation was conducted between 6-8 am. to minimize daytime evaporative loss. Frequency varied by growth stage: every 3 days at seedling stage, every 2 days at tillering stage, and daily from jointing to maturity. All operations were logged using a CR1000 datalogger, ensuring full traceability.

A water balance equation quantified effective irrigation input: $I_{net}=I_{applied}-\Delta S-E_{soil}$ (1)

where $I_{applied}$ (mm) is total irrigation depth, ΔS (mm) soil water storage change, and E_{soil} (mm) surface evaporation. Net irrigation depth fluctuations remained within ±6% during the growing season. Relative soil moisture was standardized as: $\theta_r=\frac{\theta}{\theta_{fc}}$ (2)

where θ is measured volumetric water content and θ_{fc} field capacity. These metrics ensured reliable water-gradient validation.

Morphological traits were recorded every 15 days from 15 days after transplantation (six sampling points). Measurements were conducted between 9-11 am to minimize diurnal variability. Plant height was measured using a laser rangefinder (±1 mm accuracy). Tiller number was manually counted. Basal stem diameter was measured twice using a digital vernier caliper (0.01 mm precision), and the mean was recorded.

LAI was determined using digital image analysis. Representative leaves were photographed under standardized lighting against ameld grayscale calibration background. Leaf area was calculated in ImageJ, and LAI was estimated as: $\mathrm{LAI}=\frac{\sum_{i=1}^{n}A_i}{A_{\mathrm{plot}}}$ (3)

where A_i (cm^2) is individual leaf area and A_{plot} (m^2) plot area. Fresh biomass was weighed precision of 0.1 g), oven-dried at 65°C for ≥72 h to constant weight, and dry matter accumulation rate was calculated: $R_d=\frac{W_t-W_{t-1}}{t-t_{-1}}$ (4)

All measurements were cross-validated by two operators, and raw data were stored in a structured database with automated error checking.

Simultaneously with morphological and anatomical samples were collected. Three healthy plants were selected from each treatment. Fully expanded functional leaves and basal stem internodes were fixed in FAA solution. Vacuum infiltration (-0.08 MPa, 30 min) ensured rapid fixative penetration. Samples were dehydrated in graded ethanol (70-100%), cleared in xylene, and infiltrated with paraffin (56-58°C). Sections (8 μm thickness) were cut using a rotary microtome and stained with 1% safranin (8 min) and 0.5% fast green (30 s).

Staining quality was evaluated using contrast index: $C_I=\frac{I_{\max}-I_{\min}}{I_{\max}+I_{\min}}$ (5)

$I_{\max}$ and $I_{\min}$ respectively represent the average grayscale value (unit: grayscale) of the target tissue and background area, which reflects the staining resolution ability. Define organizational fidelity T_F to measure the degree of structural loss during the preparation process:

$T_F=1-\frac{N_{\mathrm{distorted}}}{N_{\mathrm{total}}}$ (6)

$N_{\mathrm{distorted}}$ represents the number of slice segments with significant deformation, while N_{total} represents the total number of observed segments, both of which are count variables. The above formula is used for internal quality control to ensure that all slices entering the quantification stage have a reliable technical foundation. All operations are completed in a dedicated histological laboratory, with controlled environmental temperature and humidity, and the process complies with plant microscopy technical specifications.

Sections were observed under a Nikon Eclipse Ni microscope (×400). Leaf tissues (epidermis, palisade, spongy, vascular bundles) and stem tissues (thick-walled cells, parenchyma, vascular ring) were quantified using NIS-Elements software (resolution 2560 × 1920 px). Five non-overlapping fields per section were analyzed in a double-blind manner.

The proportion of thick-walled cells P_{scl} is used as a key structural parameter and is calculated using the following formula: $P_{\mathrm{scl}}=\frac{A_{\mathrm{scl}}}{A_{\mathrm{total}}}\times 100\%$ (7)

A_{scl} is the total area of thick-walled cell regions in the stem cross-section (unit: μm^2), and A_{total} is the total area of the stem cross-section (unit: μm^2). This ratio is dimensionless and reflects the relative development level of supporting tissues in the stem. The diameter D_{vb} of the vascular bundle ring is determined by fitting the minimum circumcircle: $D_{\mathrm{vb}}=2\sqrt{\frac{A_{\mathrm{vb}}}{\pi}}$ (8)

A_{vb} is the sum of the cross-sectional areas of all vascular bundles (unit: μm²), and the formula assumes that the vascular bundle rings are approximately circularly distributed, which is applicable to the anatomical configuration of the *P. purpureum* stem in this experiment. In addition, to evaluate the uniformity of tissue distribution within the field of view, the coefficient of variation CV_{field} is introduced for internal quality control: $CV_{field} = \frac{\sigma_{field}}{\bar{x}_{field}} \times 100\%$ (9)

σ_{field} is the standard deviation of a parameter in a single slice with 5 fields of view, and $\bar{x}_{field}$ is its mean. If the CV_{field} exceeds 15%, the slice is considered to have structural heterogeneity anomaly and requires additional field of view or exclusion. All calculations are automatically executed by the script, and the results are archived together with the original image. Finally, the anatomical indicators of each plant were represented as the mean of 5 visual fields and entered into the subsequent statistical model. The entire extraction process is combined with software automation and manual verification to ensure efficiency and control errors, ensuring that anatomical data has high accuracy and structural representativeness.

Results and Discussion

Cumulative irrigation input was calculated using daily irrigation volumes and meteorological data, and time-series curves were generated to verify gradient persistence and separation. Soil moisture sensor data were converted into relative soil moisture to eliminate soil texture effects. All datasets were aligned along a unified time axis to preserve strict temporal correspondence between irrigation input and soil response.

As shown in Fig. 2a, cumulative irrigation increased progressively across treatments in accordance with crop evapotranspiration (ETc), confirming dynamic amplification of water supply differences rather than static allocation. The separation among 100, 75, 50, and 25% ETc treatments widened gradually throughout the growth period, reflecting effective translation of physiological water demand into differentiated irrigation input. Soil response curves in Fig. 2b demonstrate stable stratification of relative soil moisture across treatments. The 100, 75, 50 and 25% ETc treatments maintained moisture between 0.7-0.9, 0.5-0.7, 0.3-0.5 and below 0.3, respectively. Although minor oscillations occurred due to evapotranspiration-irrigation coupling, no gradient crossover or drift was observed. Moisture variation remained within ±6% across the entire growth period. These results confirm that theoretical irrigation gradients were effectively translated into distinct and stable soil water environments. This methodological rigor addresses limitations of previous studies where insufficient gradient control confounded interpretation of plant-water relationships (Udom *et al.* 2024, Rahman *et al.* 2025). The verified stability of water treatments ensured that subsequent morphological and anatomical responses could be confidently attributed to intended irrigation regimes.

The dynamic evolution of leaf area index (LAI) and dry matter accumulation rate is presented in Fig. 3. LAI increased continuously over time across all treatments, but differences emerged among irrigation levels. As illustrated in Fig. 3a, the 75% ETc treatment slightly exceeded full irrigation in overall LAI during the active growth stage. This indicates that mild water deficit did not suppress canopy expansion and may have improved canopy architecture efficiency. The 50% ETc treatment maintained relatively high LAI, demonstrating buffering capacity under moderate stress. In contrast, the 25% ETc treatment showed clear restriction in leaf development, indicating that severe deficit exceeded compensatory capacity.

Dry matter accumulation rate patterns shown in Fig. 3b reveal earlier differentiation among treatments. The 75% ETc treatment consistently achieved the highest accumulation rate and peak value, demonstrating superior coordination between photosynthetic assimilation and biomass allocation. Although the 50% ETc treatment displayed reduced accumulation relative to 75% ETc,

its rate remained stable, indicating steady-state maintenance under constrained resources. The 25% ETc treatment exhibited persistently low accumulation, reflecting disruption of source-sink balance. The synchronization between maintained LAI and high accumulation under moderate deficit indicates that *Pennisetum purpureum* sustains productivity by preserving functional leaf area and efficient carbon conversion, rather than depending solely on abundant water supply. This forms the structural-physiological basis of its water-saving capacity.

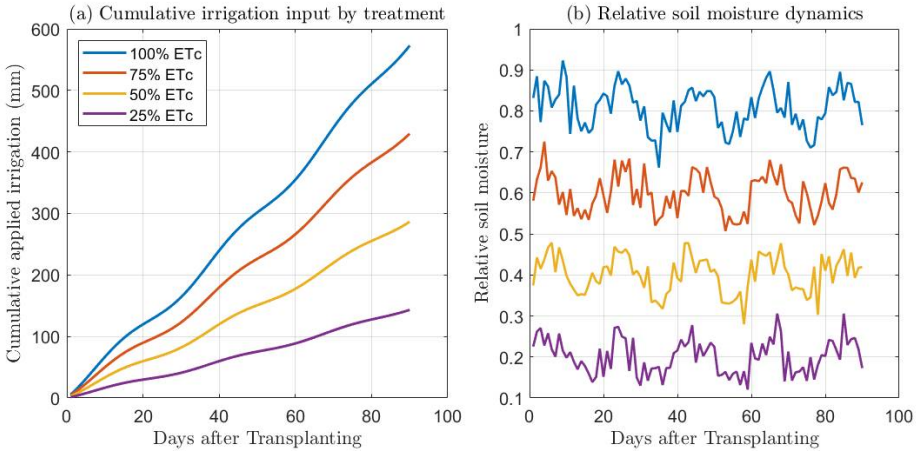

Fig. 2. Irrigation transport and soil moisture response under gradient irrigation conditions.

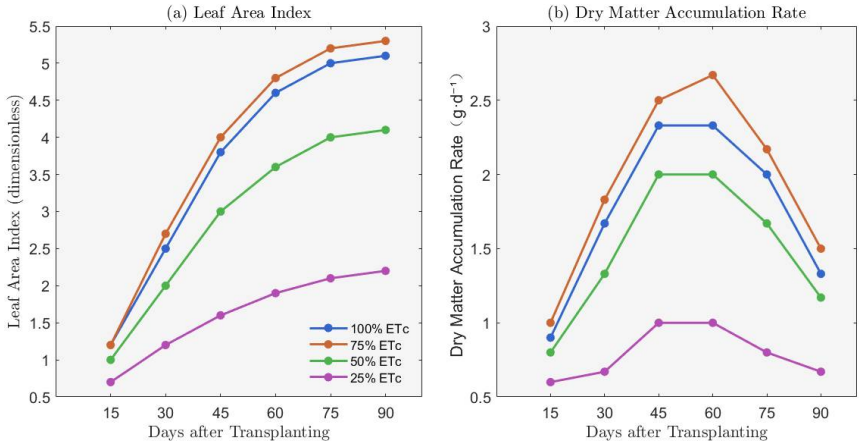

Fig. 3. Dynamic evolution of leaf development and growth rate under graded irrigation.

Water Use Efficiency (WUE) results are summarized in Table 1. WUE reached its maximum under 75% ETc (0.349 g/l), slightly exceeding full irrigation (0.339 g/l). The 50% ETc treatment maintained WUE at 0.332 g/l, remaining close to the control level. In contrast, 25% ETc declined significantly to 0.307 g/l. Biomass declined gradually with reduced irrigation, the decline between 100% and 75% ETc was minimal, indicating that mild deficit did not significantly compromise productivity. These results demonstrate coordinated physiological and structural adaptation. Under

75% ETc, reduced transpiration area and optimized stomatal regulation lowered water loss while maintaining high assimilation, enhancing productive water use (de Oliveira Gonçalves *et al.* 2022). The 50% ETc treatment further reduced water input but maintained efficient conversion through structural compensation, preventing sharp WUE decline. Severe deficit (25% ETc) exceeded tolerance limits, impairing photosynthetic organs and reducing conversion efficiency. Importantly, full irrigation did not maximize WUE, suggesting that excess water may increase non-productive transpiration. Therefore, 75% ETc represents the optimal balance between water saving and stable productivity.

Table 1. Dry matter accumulation, cumulative irrigation, effective rainfall and water use efficiency at different irrigation levels.

Irrigation level (% ETc)	Dry matter accumulation (g/m²)	Cumulative irrigation (L/m²)	Effective rainfall (L/m²)	Water use efficiency (g/l)
100	222 ± 7	570	85	0.339
75	176 ± 6	420	85	0.349
50	121 ± 5	280	85	0.332
25	69 ± 4	140	85	0.307

Morphological Plasticity Index (MPI) values under deficit treatments are presented in Fig. 4. Under 75% ETc (Fig. 4a), all morphological parameters exhibited positive MPI values. Plant height (0.18) and tiller number (0.12) showed the strongest positive responses, indicating compensatory elongation and tillering under mild deficit. Such positive plasticity across parameters suggests active phenotypic regulation rather than stress inhibition. At 50% ETc (Fig. 4b), plant height remained positive (0.08), while tiller number slightly declined (-0.05). This shift indicates beginning reallocation of resources toward maintaining vertical growth. Under 25% ETc (Fig. 4c), all MPI values turned negative; plant height decreased markedly (-0.32), and biomass production was suppressed, signaling transition from adaptive adjustment to survival response. Fig. 4 demonstrates that 75% ETc constitutes the key regulatory window where compensatory growth mechanisms are fully activated without structural collapse.

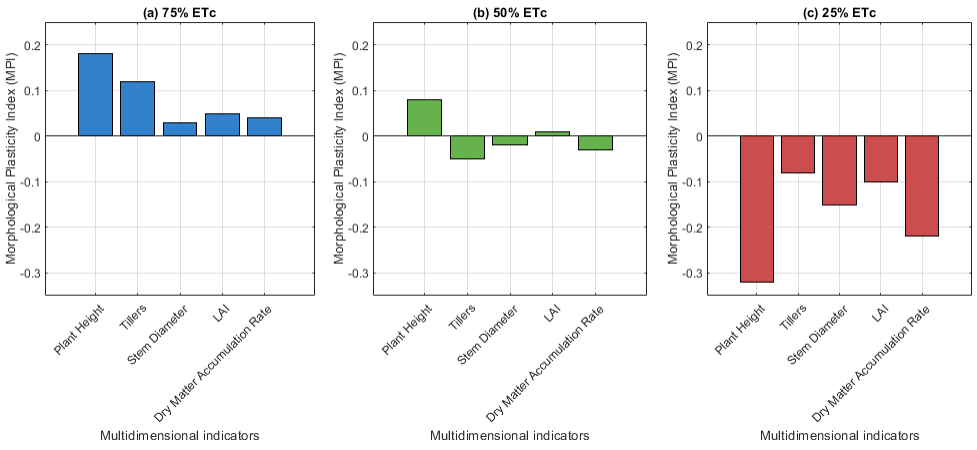

Fig. 4. Morphological plasticity index under different irrigation levels.

Quantitative anatomical traits are summarized in Table 2. The palisade/spongy tissue ratio (P/S) exhibited a non-linear response to irrigation reduction. It increased under moderate deficit and peaked at 50% ETc (1.58 ± 0.09), significantly higher than full irrigation ($p = 0.0018$). This increase indicates enhanced palisade tissue investment, which improves photosynthetic efficiency per unit leaf area. The increased P/S ratio at 50% ETc indicates greater investment in palisade parenchyma, enhancing photosynthetic efficiency per unit area while potentially reducing internal water loss via reduced air space volume. This reflects functional optimization rather than damage.

Table 2. Quantification of fitness of anatomical structures of *Pennisetum purpureum* at different irrigation levels.

Irrigation level (% ETc)	Palisade/spongy ratio (P/S)	Vascular bundle ratio (%)	P/S p-value (vs. 100% ETc)	Vascular bundle ratio p-value (vs. 100% ETc)
100	1.25 ± 0.08	18.3 ± 1.2	-	-
75	1.32 ± 0.07	18.7 ± 1.1	0.043	0.023
50	1.58 ± 0.09	18.1 ± 1.3	0.0018	0.012
25	1.41 ± 0.10	15.6 ± 1.4	0.004	0.004

Vascular bundle proportion remained stable at 75% (18.7%) and 50% ETc (18.1%), showing no significant difference from control. Only at 25% ETc it declined significantly (15.6%, $p = 0.004$). Maintenance of transport infrastructure under moderate deficit demonstrates prioritization of hydraulic safety. Thus, moderate water stress induced coordinated anatomical improved mesophyll configuration while preserving vascular capacity. Severe deficit suppressed conductive tissue development, indicating plasticity threshold exceedance.

Yield structural coupling stability was quantified as the statistical strength of association between hay yield and anatomical traits. A Pearson correlation matrix was constructed using fully processed data, and traits with $|r| \geq 0.7$ in relation to yield were selected as candidate structural stability parameters (Table 3). The variability of these parameters under different drought treatments was then examined. When the relative fluctuation remained within 10% and the linear regression with yield was statistically significant ($p < 0.05$), the trait was classified as having high coupling stability. This data-driven approach avoided subjective indicator selection by combining strong correlation and low variability criteria, directly linking functional output with anatomical structure.

Table 3. Correlation and stability between hay yield and key anatomical parameters of *Pennisetum purpureum*.

Anatomical trait (organ)	Pearson correlation	p-value	Max relative fluctuation (%)	Coupling stability
Sclerenchyma cells proportion (stem)	0.84	0.008	8.2	High
Vascular bundle area (stem)	0.62	0.032	9.5	Medium
Palisade tissue area (leaf)	0.58	0.047	12.3	Low
Spongy mesophyll area (leaf)	–0.41	0.19	15.6	Low
Epidermal thickness (leaf)	0.33	0.3	18.1	Low

As shown in Table 3, only the proportion of stem thick-walled cells satisfied all criteria for high coupling stability. It exhibited a strong positive correlation with hay yield ($r = 0.84$, $p = 0.008$), and its maximum relative fluctuation across water-deficit treatments was 8.2%, below the 10% threshold. Other parameters were excluded due to insufficient correlation (e.g., total vascular bundle area, $r = 0.62$), excessive variability (e.g., 12.3% fluctuation in palisade tissue area), or lack of statistical significance ($p > 0.05$).

These findings indicate that stem thick-walled cells (sclerenchyma) constitute the core anatomical basis for stable yield in *P. purpureum*. Mechanically, sclerenchyma fibers provide rigidity that maintains upright growth and reduces lodging risk, which is particularly important when turgor pressure declines under drought stress (Li *et al.* 2022). Hydraulically, their close association with vascular bundles helps to prevent collapse of conductive elements under negative pressure, thereby preserving water transport continuity. Physiologically, sclerenchyma development represents a structural carbon investment that, requires minimal maintenance, reflecting a long-term efficiency strategy under limited resource availability (Lambers *et al.* 2019).

The low fluctuation (8.2%) suggests that sclerenchyma development is conservative and relatively insensitive to moderate water regulation, functioning as a structural “anchor” for yield buffering. In contrast, leaf anatomical traits, although involved in photosynthetic regulation, showed greater plasticity under water stress, leading to weaker and less stable correlations with yield. This pattern, structural conservatism in supportive tissues and functional plasticity in photosynthetic tissues, reflects an adaptive strategy that balances stability and flexibility under stress conditions. Although vascular bundle area is functionally important, its moderate coupling stability ($r = 0.62$, 9.5% fluctuation) indicates higher environmental sensitivity compared to sclerenchyma. Therefore, selection for enhanced development of stem thick-walled tissue may be more effective than focusing solely on vascular traits in breeding programs targeting water-stable forage production.

Integrating results from Figs 2-4 and Tables 1-3 reveals a hierarchical adaptation strategy. At the whole-plant level, morphological plasticity, particularly compensatory tillering under 75% ETc, maintains population productivity. At the tissue level, mesophyll reorganization enhances photosynthetic efficiency while vascular transport infrastructure is preserved. At the cellular level, conservative sclerenchyma development stabilizes yield. Across all indicators, 75% ETc consistently performed optimally: highest WUE (Table 1), positive MPI (Fig. 4a), stable vascular proportion (Table 2), and strong sclerenchyma-yield coupling (Table 3). This treatment achieved approximately 25% water saving relative to full irrigation with only ~20% yield reduction, representing a favorable efficiency-stability trade-off. The 50% ETc treatment demonstrated structural resilience despite greater yield decline, as indicated by peak P/S ratio (Table 2) and maintained WUE (Table 1). However, structural collapse under 25% ETc across Figs 3-4 and Tables 1-2 confirms that this level exceeds adaptive thresholds.

The four-dimensional evaluation framework, integrating WUE, morphological plasticity, anatomical fitness, and yield-structure coupling stability, overcomes fragmentation in previous irrigation studies (Udom *et al.* 2024, Rahman *et al.* 2025). By incorporating anatomical indicators, irrigation thresholds can be set based on structural integrity rather than solely visible symptoms. Sclerenchyma proportion emerges as a measurable marker for irrigation management and breeding. Varieties with conservative supportive tissue expression may exhibit greater yield stability under water limitation.

Although gradient stability was rigorously verified (Fig. 2), validation under heterogeneous field conditions remains necessary. Root anatomical responses were not examined and may reveal additional adaptive mechanisms. Only one genotype was evaluated; genetic variation in structural

plasticity warrants investigation. Future research should integrate anatomical quantification with molecular approaches to clarify regulatory pathways coordinating leaf and stem responses under water deficit.

The results demonstrate that *Pennisetum purpureum* maintains productivity under moderate water limitation through coordinated morphological and anatomical adjustments. The optimal irrigation level was 75% ETc, characterized by highest WUE (Table 1), positive morphological plasticity (Fig. 4a), maintained vascular integrity (Table 2), and strong yield coupling with sclerenchyma proportion (Table 3). Severe deficit (25% ETc) exceeded structural plasticity limits, resulting in functional collapse. The four-dimensional evaluation framework established here provides a scientific basis for structure-oriented precision irrigation and supports sustainable forage production under water-limited conditions.

References

Braga RM, Melo DM, Melo MA, Freitas JC and Boateng AA 2022. Effect of pretreatment on pyrolysis products of *Pennisetum purpureum* Schum. by Py-GC/MS. J. Therm. Anal. Calorim. **147**(12): 6655-6663.

Clark PD, Otutu JO, Asiagwu KA, Ndukwe GI and Idibie CA 2023. Investigating the feasibility of utilizing *Pennisetum purpureum* leaves waste as a sustainable dye: Extraction, characterization and application on textile. Sci. Afr. **22**(3): 231-246.

Dios-León GE, Ramos-Juárez JA, Izquierdo-Reyes F, Joaquín-Torres BM and Meléndez-Nava F 2022. Productive performance and nutritional value of *Pennisetum purpureum* cv. Cuba CT-115 grass at different regrowth ages. Rev. Mex. Cienc. Pecu. **13**(4): 1055-1066.

de Oliveira Gonçalves M, Carpanez TG, Silva JB, Otenio MH, de Paula VR and de Mendonça HV 2022. Biomass production of the tropical forage grass *Pennisetum purpureum* (BRS Capiaçu) following biofertilizer application. Waste Biomass Valorization **13**(4): 2137-2147.

Ho PY, Koh YC, Lu TJ, Liao PL and Pan MH 2023. Purple Napiergrass (*Pennisetum purpureum* Schumach) hot water extracts ameliorate high-fat diet-induced obesity and metabolic disorders in mice. J. Agric. Food Chem. **71**(51): 20701-20712.

Ikpeseni SC, Orugba HO, Efetobor UJ, Sada SO, Ekpu M, Amagre ME and Owamah HI 2025. Pyrolysis characteristics and kinetics of the thermal degradation of elephant grass (*Pennisetum purpureum*): a comparative analysis using the Flynn–Wall–Ozawa and the Kissinger–Akahira–Sunose methods. Environ. Dev. Sustain. **27**(5): 10549-10567.

Ikpeseni SC, Sada SO, Efetobor UJ, Orugba HO, Ekpu M, Owamah HI, Chukwuneke JL, Oyebisi S and Onochie UP 2024. Optimization of bio-oil production parameters from the pyrolysis of elephant grass (*Pennisetum purpureum*) using response surface methodology. Clean Energy **8**(5): 241-251.

Ikyume TT, Shaahu DT, Enebi B, Tor-Anyyin DD, Anzewu OE, Opawoye FA, Abba JJ and Ewetade RO 2025. Effect of fertilizer types on yield and quality of napier (*Pennisetum purpureum*) grass established in makurdi and harvested at different growth stages during the wet season. Fudma J. Sci. **9**(5): 34-42.

Jabessa T, Bekele K, Tesfaye G and Amare Z 2022. Evaluation of elephant grass (*Pennisetum purpureum* L) accessions for their agronomic performances in lowland areas of Guji Zone, Southern Oromia, Ethiopia. Am. J. Biol. Environ. Stat. **8**(1): 31-35.

Johannes LP, Minh TT and Xuan TD 2024. Elephant grass (*Pennisetum purpureum*): a bioenergy resource overview. Biomass **4**(3): 625-646.

Kalebbi M, Nohong B and Utamy RF 2024. Morphology traits and dry matter yield of *Pennisetum purpureum* Pakchong 1 fertilized by liquid organic fertilizer. Hasanuddin J. Anim. Sci. **6**(1): 38-46.

Lambers H, Oliveira RS and Pons TL 2019. Growth and allocation. *In*: Plant Physiological Ecology. Springer, Cham. pp. 385-449.

Li Z, Yu X and Jia G 2022. The anatomical structure of woody plants in arid habitats is closely related to nonstructural carbohydrates storage. For. Ecosyst. **9**: 100073.

Maldonado-Méndez JD, Guerra-Medina CE, Avendaño-Arrazate CH, Gálvez-Marroquín LA and Ariza-Flores R 2023. Morphological characterization of elephant grass (*Pennisetum purpureum* Schumach) ecotypes collected in Chiapas, Mexico. Agro Productividad **16**(1): 33-43.

Mijena D and Getiso A 2023. Adaptation and herbage yield performance of *Pennisetum purpureum* grass genotypes in the rift valley of Ethiopia. Int. J. Agric. Vet. Sci. **5**(4): 33-42.

Mijena D, Getiso A, Islam MR and Shafi KM 2023. Herbage yield evaluation of *Pennisetum purpureum* grass genotypes. Int. J. Agric. Vet. Sci. **5**(4): 64-74.

Mohamad SS, Kamaruddin NA and Ting JY 2022. Study on chemical composition of napier pak chong (*Pennisetum purpureum* x *Pennisetum glaucum*) harvested at different growth stages. J. Agrobiotec. **13**(1S): 24-30.

Oluwadele JF, Ekeocha AH, Aganga AA, Tawose OM, Odumboni A, Ofodome CI and Akinlabi EY 2024. Effects of feeding *Pennisetum purpureum* silage supplemented with selected farm residues on growth performance and meat quality of west African dwarf rams. SVU-Int. J. Agric. Sci. **6**(3): 190-196.

Putra B, Gopar RA, Surachman M, Darmawan IW, Maulana S and Prasetya B 2024. Nutrient value and *in vitro* digestibility of *Pennisetum purpureum* cv. Mott under varying gamma irradiation doses in acidic soil. Trop. Anim. Sci. J. **47**(2): 206-214.

Qohar AF, Utami ET, Chalisty VD, Nuraeni N, Mugiarto M, Teguh M and Sitohang S 2023. Pengenalan hijuan pakan ternak rumput odot (*Pennisetum purpureum* cv. Mott) di Desa Ambalkumolo Kecamatan Buluspesantren. J. Pengabdian Masy. Nusantara **4**(3): 2215-2220.

Rahman ME, Uddin MK, Shamsuzzaman SM, Mahmud K, Shukor MY, Ghani SS, Nabayi A, Sadeq BM, Chompa SS, Akter A and Halmi MI 2025. Utilizing NPKS fertilizer for the enhancement of *Pennisetum purpureum* growth and phytoremediation of arsenic in treatment wetland. Int. J. Phytorem. **27**(7): 972-990.

Silva SP, Montanha GS, Devechio FD and Marques JP 2024. Liming and plastering modify root anatomy in *Pennisetum purpureum* Schum. Int. J. Plant Biol. **15**(2): 442-451.

Udom NR, Ogwo PA and Uchendu UI 2024. Crude oil remediation potentials of *Pennisetum purpureum* in oil producing communities of Akwa Ibom State, Nigeria. J. Health Appl. Sci. Manage. **7**(2): 245-254.

Veraque MJ and Gorne N 2023. Response of napier grass (*Pennisetum purpureum* Schum.) to different levels of nitrogen fertilizer in the Philippines. Ann. Trop. Res. **45**(1): 61-71.

(Manuscript received on 10 March, 2026; revised on 09 March, 2026)